

A Comparative Study of the Therapeutic Potential of Mesenchymal Stem Cells and Limbal Epithelial Stem Cells for Ocular Surface Reconstruction

VLADIMIR HOLAN,^{a,b} PETER TROŠAN,^{a,b} CESTMIR CEJKA,^{a,c} ELISKA JAVORKOVA,^{a,b} ALENA ZAJICOVA,^a BARBORA HERMANKOVA,^{a,b} MILADA CHUDICKOVA,^{a,b} JITKA CEJKOVA^a

Key Words. Limbal stem cells • Mesenchymal stem cells • Alkali-injured ocular surface • Corneal regeneration • Stem cell-based therapy

ABSTRACT

Stem cell-based therapy has become an attractive and promising approach for the treatment of severe injuries or thus-far incurable diseases. However, the use of stem cells is often limited by a shortage of available tissue-specific stem cells; therefore, other sources of stem cells are being investigated and tested. In this respect, mesenchymal stromal/stem cells (MSCs) have proven to be a promising stem cell type. In the present study, we prepared MSCs from bone marrow (BM-MSCs) or adipose tissue (Ad-MSCs) as well as limbal epithelial stem cells (LSCs), and their growth, differentiation, and secretory properties were compared. The cells were grown on nanofiber scaffolds and transferred onto the alkali-injured eye in a rabbit model, and their therapeutic potential was characterized. We found that BM-MSCs and tissue-specific LSCs had similar therapeutic effects. Clinical characterization of the healing process, as well as the evaluation of corneal thickness, re-epithelialization, neovascularization, and the suppression of a local inflammatory reaction, were comparable in the BM-MSC- and LSC-treated eyes, but results were significantly better than in injured, untreated eyes or in eyes treated with a nanofiber scaffold alone or with a nanofiber scaffold seeded with Ad-MSCs. Taken together, the results show that BM-MSCs' therapeutic effect on healing of injured corneal surface is comparable to that of tissue-specific LSCs. We suggest that BM-MSCs can be used for ocular surface regeneration in cases when autologous LSCs are absent or difficult to obtain. *STEM CELLS TRANSLATIONAL MEDICINE* 2015;4:1–12

SIGNIFICANCE

Damage of ocular surface represents one of the most common causes of impaired vision or even blindness. Cell therapy, based on transplantation of stem cells, is an optimal treatment. However, if limbal stem cells (LSCs) are not available, other sources of stem cells are tested. Mesenchymal stem cells (MSCs) are a convenient type of cell for stem cell therapy. The therapeutic potential of LSCs and MSCs were compared in an experimental model of corneal injury and healing was observed following chemical injury. MSCs and tissue-specific LSCs had similar therapeutic effects. The results suggest that bone marrow-derived MSCs can be used for ocular surface regeneration in cases when autologous LSCs are absent or difficult to obtain.

INTRODUCTION

Severe injuries or defects of the cornea represent among the most common causes of decreased quality of vision or even blindness. In many cases, penetrating keratoplasty is performed as the first treatment option. However, if the corneal damage is more extensive and the limbal region is involved, the defect can lead to limbal stem cell deficiency (LSCD). In such cases, corneal transplantation alone is not a sufficient treatment method. The only effective way to treat LSCD is by the transplantation of whole limbal tissue or the transfer of limbal epithelial stem cells (LSCs). Although beneficial

effects of limbal transplantation have been reported [1–3], the shortage of limbal tissue and a strong immune response to a limbal allograft are the main obstacles to such treatment protocols. Therefore, a more promising treatment method is offered by LSC transplantation. The first encouraging results from LSC transplantation have been published [4–6]. Since LSCs represent a relatively small population of limbal cells that are difficult to isolate and prepare in sufficient quantities, other stem cell sources are being explored and tested to treat LSCD.

An alternative source of stem cells for ocular surface regeneration and the treatment of LSCD is mesenchymal stem cells (MSCs). These cells can

^aInstitute of Experimental Medicine, Academy of Sciences of the Czech Republic, Prague, Czech Republic; ^bFaculty of Natural Science, Charles University, Prague, Czech Republic; ^cCzech Technical University in Prague, Faculty of Biomedical Engineering, Kladno, Czech Republic

Correspondence: Vladimír Holan, Ph.D., Institute of Experimental Medicine, Academy of Sciences of the Czech Republic, Videnska 1083, 14220, Prague 4, Czech Republic. Telephone: 420 241063226; E-Mail: holan@biomed.cas.cz

Received March 3, 2015; accepted for publication June 15, 2015.

©AlphaMed Press
1066-5099/2015/\$20.00/0

<http://dx.doi.org/10.5966/sctm.2015-0039>

be obtained relatively easily in a sufficient amount from various types of tissues (e.g., bone marrow, adipose tissue) and expanded *in vitro* for autologous application. It has been shown that MSCs retain their differentiation potential during *in vitro* expansion and that they can differentiate into various cell types [7], including cells expressing corneal epithelial cell markers [8, 9]. The first results of using MSCs for ocular surface healing in small animal models have been published [9, 10]. We have shown in mice [11] and rabbits [12] that MSCs grown on a nanofiber scaffold and transferred onto the damaged ocular surface significantly inhibit the local inflammatory reaction and support the healing process.

Although LSCs and MSCs have different origins, they share comparable immunoregulatory properties *in vitro* [13]. Similarly, numerous common properties have been described for tissue-specific stem cells isolated from different organs [14]. Comparative studies on MSCs prepared from bone marrow and other sources have shown many similarities but also some differences [15, 16]. For the treatment of ocular surface injuries and LSCD, both tissue-specific LSCs and MSCs isolated from the bone marrow (BM-MSCs) or adipose tissue (Ad-MSCs) have been proposed and tested. In these studies, MSCs proved to be a promising cell type to support the healing of the damaged ocular surface [9–12, 17–19]. However, so far, there is no direct evidence that MSCs can support the healing and regeneration of damaged corneal tissue as effectively as the tissue-specific LSCs. Therefore, in the present study, we used a well-established model of the alkali-damaged ocular surface in rabbits and directly compared the regenerative and reparative potential of tissue-specific LSCs and MSCs derived from bone marrow or adipose tissue. On the basis of several evaluated parameters, we show the therapeutic potential of BM-MSCs for the treatment of damaged ocular surface is comparable to that of tissue-specific LSCs, and, thus, BM-MSCs can be used therapeutically as a convenient source of stem cells to support healing of the wounded cornea.

MATERIALS AND METHODS

Animals and Alkali-Induced Corneal Damage

Adult, female New Zealand white rabbits (2.5–3.0 kg) obtained from Velaz Ltd. (Prague, Czech Republic, <http://www.velaz.cz>) were used in the experiments. Rabbits were anesthetized by an intramuscular injection of a 1:1 mixture of xylazine hydrochloride 2% (0.2 ml/kg body weight; Rometar; Spofa, Prague, Czech Republic, <http://www.spofa.cz>) and ketamine hydrochloride 5% (1 ml/kg body weight; Narkamon; Spofa). The right corneas of anesthetized rabbits were injured by dropping 0.25N sodium hydroxide (NaOH) on the corneal surface (10 drops during 1 minute, alkali injuring the whole cornea, including the limbal region), then the eyes were immediately rinsed with an excess of tap water. After the alkali injury and awakening from the anesthesia, the rabbits were treated with analgesia (ketoprofen, 1.0 mg/kg *i.m.*) 2 times daily for 5 days. All experiments were conducted according to the Association for Research in Vision and Ophthalmology Statement on the Use of Animals in Ophthalmic and Vision Research and were approved by the local ethics committee.

Isolation of LSCs and MSCs

LSCs were obtained by the enzymatic digestion of limbal tissue, as we have described in a mouse model [20]. In brief, limbal

tissue was cut with scissors and subjected to 10 short (10 minutes each) trypsinization cycles. The released cells were harvested after each cycle, centrifuged (8 minutes at 250g), and resuspended in Roswell Park Memorial Institute (RPMI) 1640 medium (Sigma-Aldrich Corp., St. Louis, MO, <http://www.sigmaaldrich.com>) containing 10% fetal calf serum (FCS; Sigma-Aldrich), antibiotics (100 U/ml penicillin, 100 µg/ml streptomycin), and 10 mM HEPES buffer. The cells were seeded in 25-cm² tissue culture flasks (Corning Inc., Schiphol-Rijk, The Netherlands, <http://www.corning.com>). For characterization of the cells and for their transfer onto a nanofiber scaffold, cells grown *in vitro* for 2–3 weeks (third passage) were used.

BM-MSCs were isolated from the femurs of rabbits. The bone marrow was flushed out, a single-cell suspension was prepared by homogenization, and the cells were seeded at a concentration of 4×10^6 cells per milliliter in Dulbecco's modified Eagle's medium (DMEM; Sigma-Aldrich) containing 10% FCS, antibiotics (100 U/ml penicillin, 100 mg/ml streptomycin), and 10 mM HEPES buffer in 25-cm² tissue culture flasks (Corning). After a 48-hour incubation, the nonadherent cells were washed out and the adherent cells were cultured with a regular exchange of the medium and passaging of the cells to maintain their optimal concentration. The cells were characterized and used at the third passage.

Ad-MSCs were isolated from subcutaneous adipose tissue. The tissue was cut into small pieces with scissors and incubated in 1 ml of Hanks' balanced salt solution containing 10 mg/ml collagenase type I (Sigma-Aldrich) for 60 minutes at 37°C with gentle agitation. Then the collagenase was diluted with complete DMEM. The cells were filtered and centrifuged at 250g for 8 minutes. The upper adipose layer was removed, the cells were centrifuged, resuspended in 6 ml complete DMEM (4×10^6 cells per milliliter), and seeded in 25-cm² tissue culture flasks (Corning). After incubation for 48 hours, the cells were washed with medium to remove nonadherent cells and cell debris, and cultured under standard conditions. Ad-MSCs were used in passages 3 and 4.

Stem Cell Growth, Differentiation, and Gene Expression

To show the morphology of MSCs and LSCs, the cells were grown on glass cover slips, fixed with paraformaldehyde, and incubated with Alexa Fluor 568 phalloidin (Invitrogen/Thermo Fisher Scientific Inc., Paisley, U.K., <http://www.thermoscientific.com>) to label F actin. The nuclei were visualized by using 4',6-diamidino-2-phenylindole (DAPI) fluorescent dye (Invitrogen). Images were taken by a laser scanning confocal microscope (Zeiss International, Jena, Germany, <http://www.zeiss.com>). For characterization of their growth properties, cells were seeded (1×10^4 cells per well) in 500 µl of complete DMEM in 48-well tissue culture plates (Nunc/Thermo Fisher Scientific Inc., Roskilde, The Netherlands, <http://www.thermoscientific.com>), and the growth of the cells was determined after 3-, 24-, and 48-hour cultivation using the WST assay, as we have described [21]. In brief, WST-1 reagent (Roche Diagnostics, Mannheim, Germany, <http://www.roche.de>) was added to each well to form formazan. The plates were then incubated for another 4 hours, and the absorbance was measured by spectrophotometry. The assay is based on the ability of living cells to use mitochondrial dehydrogenases to cleave tetrazolium salts into water-soluble formazan, which is then measured by spectrophotometry. To compare the growth

of stem cells on plastic or on a nanofiber scaffold, MSCs and LSCs were seeded (4×10^4 cells per well) in 700 μ l DMEM in 24-well tissue culture plates (Corning) directly into wells or onto a nanofiber scaffold fixed into CellCrown TM24 inserts (Scaffdex Ltd., Tampere, Finland, <http://www.scaffdex.com>). The growth of cells was determined after 48 hours by the WST assay.

The ability of stem cells to differentiate into adipocytes was determined using specific adipogenic medium containing 0.1 μ M dexamethasone, 0.5 mM 3-isobutyl-1-methylxanthine, 0.1 mM indomethacine, and 0.5 μ g/ml insulin, as we described previously [22]. The differentiation of the cells was confirmed by staining with Oil Red O and by quantifying the expression of the adipocyte-specific genes for adiponectin (*ADPC*) and peroxisome proliferator-activated receptor γ (*PPAR* γ) using real-time polymerase chain reaction (PCR).

The expression of genes for the immunoregulatory molecules indoleamine-2,3-dioxygenase (*IDO-2*), cyclooxygenase-2 (*Cox-2*) and inducible nitric oxide synthase (*iNOS*), and for hepatocyte growth factor (*HGF*), transforming growth factor- β (*TGF- β*), and vascular endothelial growth factor (*VEGF*) was determined in unstimulated and lipopolysaccharide (*LPS*)-stimulated MSCs and LSCs. In these experiments, the cells (4×10^4 cells per well) were cultured in 700 μ l of DMEM for 48 hours in 24-well tissue culture plates (Corning) with or without 5 μ g/ml *LPS*, and the expression of the genes was determined by real-time PCR, as described below.

Nanofiber Scaffolds

Nanofiber scaffolds were prepared from the biocompatible polymer poly(L-lactic acid) (*PLA*) by a needleless electrospinning procedure, as we have described [23]. In brief, *PLA* polymer was dissolved in chloroform and two other solvents, 1,2-dichloroethane and ethyl acetate, were added to this solution. The mixture was stirred until a homogenous polymer solution was obtained. The modified needleless Nanospider technology (Elmarco s.r.o., Liberec, Czech Republic, <http://www.elmarco.com>), in which polymeric jets are spontaneously formed from liquid surfaces on a rotating spinning electrode, was used for the preparation of the nanofibers. In this study, nanofiber material with a mass per unit area of 10 g/m² and with a nanofiber diameter ranging from 290 to 539 nm was used. The morphology of the nanofibers and their nanofibrous architecture were analyzed using scanning electron microscopy and shown previously [11, 21].

Stem Cell Growth on Nanofiber Scaffold and Cell Transfer

Nanofiber scaffolds were cut into squares (approximately 1.5 \times 1.5 cm) and fixed into CellCrown TM24 inserts (Scaffdex). The inserts with nanofibers were transferred into 24-well tissue culture plates (Corning). Stem cells (3×10^5) in 700 μ l of complete DMEM were transferred into each well. The plates were incubated for 24 hours to allow the cells to adhere to the scaffold.

For stem cell transfer, nanofiber scaffolds seeded with stem cells were transferred within 1 hour after the injury with the cell side facing down on the damaged ocular surface. The scaffolds were sutured to the conjunctiva with four interrupted sutures using 11.0 Ethilon (Ethicon, Johnson & Johnson, Livingston, U.K., <http://www.ethiconproducts.co.uk>). The eyelids were closed by tarsorrhaphy using 1 suture of Resolon 7.0 (Resorba Medical GmbH, Nuremberg, Germany, <http://www.resorba.com>) for 72

hours. An ophthalmic ointment compound containing bacitracin and neomycin (Ophthalmo-Framykoin; Zentiva Group, Prague, Czech Republic, <http://www.zentiva.com>) was applied on the ocular surface for 3 days. The nanofiber scaffolds were removed from the ocular surface on day 3 after the operation. The animals were sacrificed following an i.v. injection of thiopental anesthesia (30 mg/kg thiopental; Spofa) after premedication with an intramuscular injection of xylazine hydrochloridum/ketaminum hydrochloridum. Each experimental group involved six rabbits (i.e., six experimental eyes). In all experiments with alkali injury, the corneas of healthy rabbit eyes served as controls.

Immunohistochemistry

After sacrificing the animals, the eyes were enucleated and the anterior eye segment dissected out and quenched in light petroleum chilled with an acetone-dry ice mixture. Sections were cut on a cryostat and transferred onto glass slides. Subsequently, the cryostat sections were fixed in acetone at 4°C for 5 minutes. For the immunohistochemical detection of cells staining for CD3, *iNOS*, *VEGF*, or the cytokeratins K3 and K12 (*K3/12*), the following primary monoclonal antibodies (mAbs) were used: anti-CD3 (Abcam, Cambridge, U.K., <http://www.abcam.com>), anti-*iNOS* (BD Biosciences, San Jose, CA, <http://www.bdbiosciences.com>), anti-caspase-3 (Abcam), anti-*K3/12* (Abcam), and anti-*VEGF* (Abcam). The binding of the primary antibodies was demonstrated using the horseradish peroxidase/3,3'-diaminobenzidine (HRP/DAB) Ultra Vision detection system (Thermo Fisher Scientific) following the instructions of the manufacturer. Individual steps involved the following: hydrogen peroxide block (15 minutes), ultra V block (5 minutes), incubation with the primary antibody (60 minutes), incubation (10 minutes) with biotinylated goat anti-mouse IgG secondary antibody (Thermo Fisher Scientific) and peroxidase-labeled streptavidin incubation (10 minutes). Visualization was performed using a freshly prepared DAB substrate-chromogen solution. Cryostat sections in which the primary antibodies were omitted from the incubation media served as negative controls. Some sections were counterstained with Mayer's hematoxylin.

The counting of cells positive for CD3 and *iNOS* in the corneal stroma and for caspase-3 in the corneal epithelium was performed by an examiner without prior knowledge of the experimental procedure. Three randomly chosen fields of corneal sections (of the same field size and the same microscope magnification) from six corneas of each experimental animal group were used. For each cornea, the mean value from the three fields was calculated.

Determination of Corneal Thickness

Changes of corneal transparency after the injury and during healing were examined according to the measurement of the central corneal thickness (taken as an index of corneal hydration). The central corneal thickness was measured in anesthetized animals using an ultrasonic pachymeter SP-100 (Tomey Corp., Nagoya, Japan, <http://www.tomey.com>) in the corneal center. The corneal thickness was measured in the same corneas before alkali injury (corneas of healthy eyes) and on days 5 and 12 after the injury (all experimental groups). Each cornea was measured four times and the mean value of the thickness (in μ m) was computed.

Determination of Corneal Neovascularization and Re-epithelialization

For the evaluation of corneal neovascularization, the number of vessels was counted in each 60° sector of the corneal surface. The mean value and standard deviation were determined from six eyes in each group.

To characterize corneal re-epithelialization, postfixed cryostat sections of the corneas were stained with a mAb directed against the corneal epithelial cell-associated cytokeratins K3 and K12, using hematoxylin and eosin stain for counterstaining. The images were evaluated microscopically. For the quantification of re-epithelialization, the expression of genes for K3 and K12 was determined by real-time PCR in healthy, injured and treated corneas.

Detection of Gene Expression by Real-Time PCR

The expression of genes in cultured cells or in control and treated corneas was determined by quantitative real-time PCR. The corneas or cultured stem cells were transferred into Eppendorf tubes containing 500 μ l TRI Reagent (Molecular Research Center Inc., Cincinnati, OH, <http://mrcgene.com>). The details of RNA isolation, transcription, and the PCR parameters have been described previously [24]. In brief, total RNA was extracted using TRI Reagent according to the manufacturer's instructions. Total RNA (1 μ g) was treated using deoxyribonuclease I (Promega Corp., Madison, WI, <http://www.promega.com>) and subsequently used for reverse transcription. The first-strand cDNA was synthesized using random primers (Promega) in a total reaction volume of 25 μ l using Moloney murine leukemia virus reverse transcriptase (Promega).

Quantitative real-time PCR was performed using a StepOne-Plus real-time PCR system (Thermo Fisher Scientific). The relative quantification model with efficiency correction was applied to calculate the expression of the target gene in comparison with glyceraldehyde 3-phosphate dehydrogenase (GAPDH) used as the housekeeping gene. The following primers were used for amplification: GAPDH: 5'-CCCAACGTCTGTCGTG (sense), 5'-CCGACCCAGACGTACAGC (antisense); K3: 5'-GAACAAGGTCCTG-GAGACCA (sense), 5'-TTGAAGTCTCC ACCAGGTC (antisense); K12: 5'-AGGAGGTGGTGAATGGTGAG (sense), 5'-GTTGTTCCAGGAGCAAAA (antisense); ADPC: 5'-ACCAGGACAAGAACGTGGAC (sense), 5'-TGGAGATGGAATCGTTGACA (antisense); PPAR γ : 5'-AGTCGCCATCC GCATCTT (sense), 5'-ATCTCATGGACCCG-TACTTG (antisense); IDO-2: 5'-GTTTC CTTGGCTCGTTGG (sense), 5'-CCTTTTCTGAAAGGATAAATCTCG (antisense); iNOS: 5'-AGG-GAGTGTGTTCCAGGTG (sense), 5'-TCCTCAACCTGCTCCTCACT (antisense); Cox-2: 5'-ACATCGTCAATAGCATTC (sense), 5'-TAGTAG-GAGAGGTT GAGA (antisense); TGF- β 1: 5'-GCCTGCAAGTGCTAAGT-TAC (sense), 5'-TGCTG CATTCTGGTACAGC (antisense); HGF: 5'-AGGCAGCTATAAGGGAAACAGTG (sense), 5'-ATGGAACCTCAGGGCT-GAC (antisense); and VEGF: 5'-CGAGACCTTGGTG GACATCT (sense), 5'-ATCTGCATGGTGACGTTGAA (antisense). The PCR parameters included denaturation at 95°C for 3 minutes, then 40 cycles at 95°C for 20 seconds, annealing at 60°C for 30 seconds, and elongation at 72°C for 30 seconds. Fluorescence data were collected at each cycle after an elongation step at 80°C for 5 seconds and were analyzed using StepOne Software, version 2.2.2 (Thermo Fisher Scientific). Each individual experiment was performed in triplicate.

Statistical Analysis

Analysis of the data showed a normal distribution and the results are expressed as mean \pm SD. Comparisons between two groups

were made using Student *t* test, and multiple comparisons were analyzed by analysis of variance. A value of $p < .05$ was considered statistically significant.

RESULTS

Growth, Differentiation, and Gene Expression of Rabbit MSCs and LSCs

The morphology of BM-MSCs, Ad-MSCs, and LSCs growing on glass cover slips in vitro is shown in Figure 1A. All three cell types adhered to plastic and glass surfaces and had a typical fibrocyte-like shape. The cells had similar growth characteristics when cultured on plastic (Fig. 1B) and proliferated comparably on a nanofiber scaffold (Fig. 1C). When all three cell types were cultured in a specific adipogenic differentiation medium, the highest differentiation potential was recorded in BM-MSCs, as demonstrated microscopically (Fig. 1D) and also according to the expression of genes for the adipocyte markers ADPC and PPAR γ determined by real-time PCR (Fig. 1E).

To test the ability of BM-MSCs, Ad-MSCs, and LSCs to produce basic immunoregulatory molecules and growth factors, the cells were cultured for 48 hours unstimulated or stimulated with LPS, and the expression of genes for IDO-2, Cox-2, iNOS, TGF- β , HGF, and VEGF was determined by real-time PCR. As shown in Figure 2, some of these genes were expressed spontaneously and comparably in all cell types, while other factors were produced preferentially in only some cell populations or only after stimulation with LPS.

Immunohistochemical Detection of CD3⁺, iNOS⁺, and Caspase-3⁺ Cells in Alkali-Injured and Stem Cell-Treated Corneas

The presence of CD3⁺ cells (Fig. 3A) or cells expressing iNOS (Fig. 3B) or caspase-3 (Fig. 3C) was very low or absent in healthy control corneas. After alkali injury, the corneas were strongly infiltrated with CD3⁺ cells (Fig. 3D) and the expression of iNOS (Fig. 3E) was high. Similarly, the number of apoptotic caspase-3⁺ cells was high in the remaining islands of the corneal epithelium (Fig. 3F). The infiltration of corneas with CD3⁺ cells (Fig. 3G) or the presence of iNOS⁺ (Fig. 3H) or caspase-3⁺ (Fig. 3I) cells was slightly decreased in injured corneas treated with cell-free nanofiber scaffolds. However, after the treatment of injured corneas with stem cell-seeded nanofibers (Fig. 3J–3R), the numbers of CD3⁺, iNOS⁺, or caspase-3⁺ cells were significantly decreased. The expression of caspase-3 in apoptotic cells, which was high in the remaining islands of the corneal epithelium in untreated injured corneas (Fig. 3F, arrow), was only weakly expressed in the epithelium of corneas treated with a nanofiber scaffold seeded with BM-MSCs (Fig. 3L, arrow) or LSCs (Fig. 3R, arrow). The number of CD3⁺ cells (Fig. 3V) as well as cells expressing iNOS (Fig. 3W) or caspase-3 (Fig. 3X) was counted in defined fields of corneal sections for each experimental group. The graphs show that the numbers of CD3⁺, iNOS⁺, or caspase-3⁺ cells, which were high in untreated injured corneas or corneas treated with cell-free nanofiber scaffolds, were significantly decreased in the groups treated with stem cell-seeded nanofibers.

Corneal Thickness After Alkali-Injury and Treatment With MSCs and LSCs

The central corneal thickness of healthy corneas was about 380 μ m (Fig. 4). Shortly after alkali injury, the corneal thickness increased (as a result of hydration) more than twofold and remained high on day 5

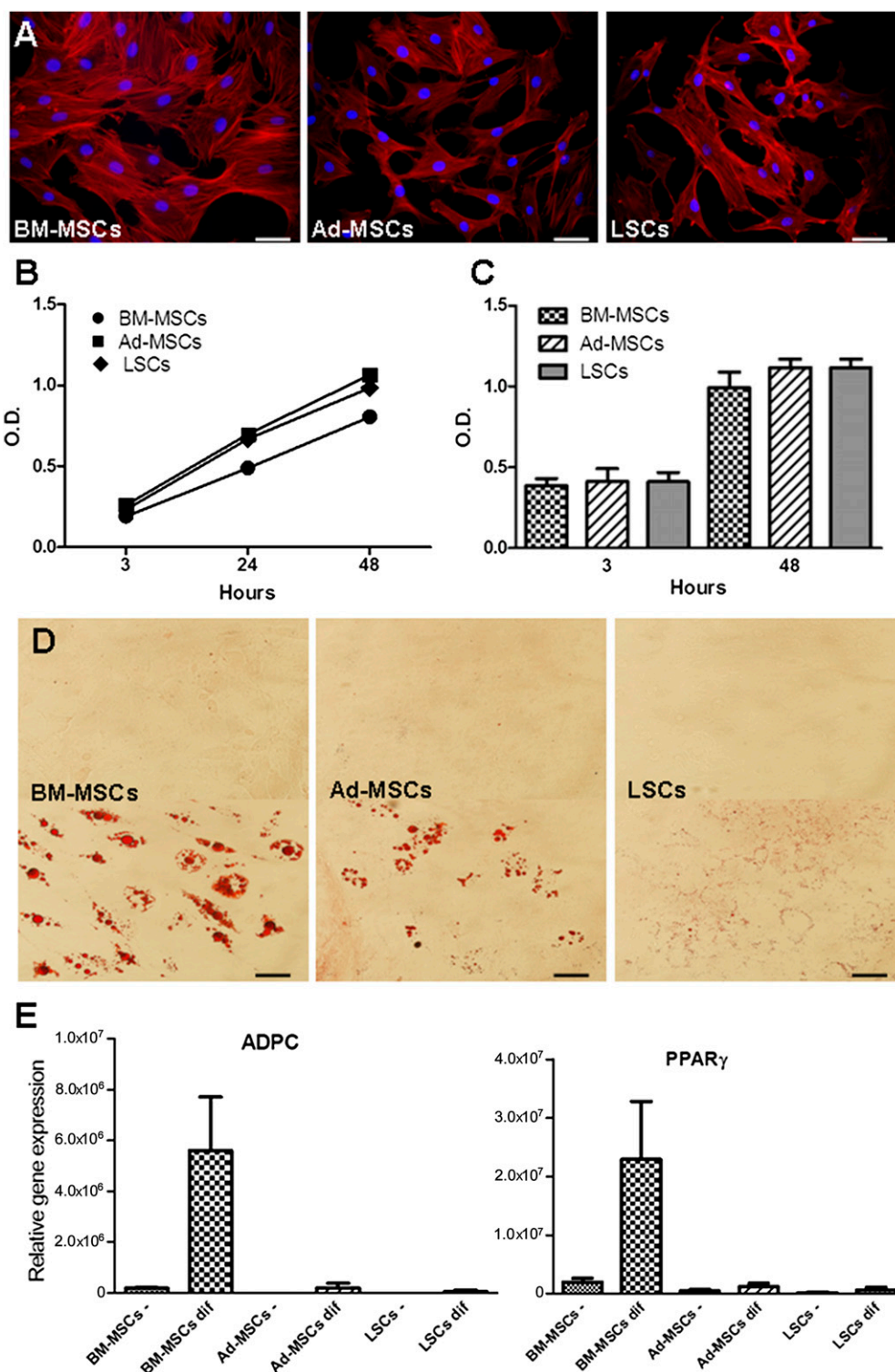


Figure 1. Characterization of BM-MSCs, Ad-MSCs, and LSCs. **(A):** The morphology of the cells is shown by staining for F-actin with phalloidin (red filaments). The nuclei are blue (4',6-diamidino-2-phenylindole [DAPI] staining). Scale bars = 200 μ m. **(B–E):** The growth of cells on plastic **(B)** or on a nanofiber scaffold **(C)** was determined by the WST assay. The ability of cells to differentiate into adipocytes was characterized microscopically **(D)**, upper: undifferentiated cells; lower: cells in differentiation medium) or according to the expression of the *ADPC* and *PPAR γ* genes detected by real-time polymerase chain reaction **(E)**. Each bar represents the mean \pm SD from three determinations. Abbreviations: Ad-MSC, adipose tissue-derived mesenchymal stem cell; *ADPC*, adiponectin gene; BM-MSC, bone marrow-derived mesenchymal stem cell; dif, differentiation medium; LSC, limbal epithelial stem cell; o.d., optical density (absorbance); *PPAR γ* , peroxisomeproliferator-activated receptor γ .

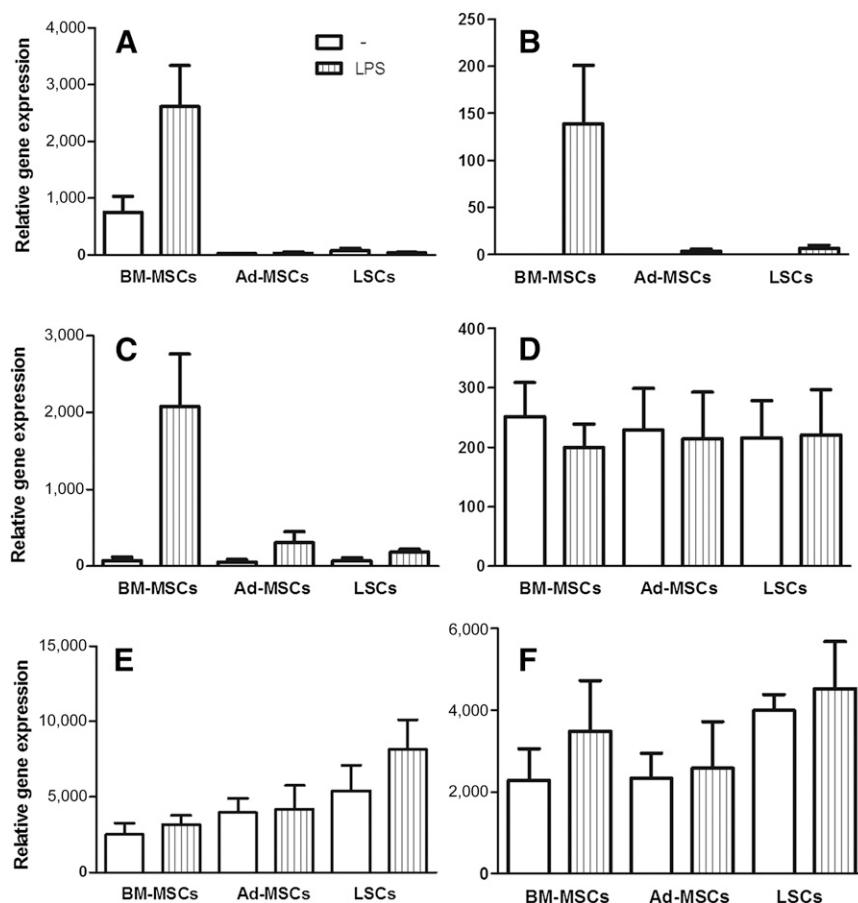


Figure 2. Expression of genes for immunoregulatory molecules and growth factors by BM-MSCs, Ad-MSCs, and LSCs. (A–F): The cells were cultured for 48 hours unstimulated or stimulated with LPS and the expression of genes for indoleamine-2,3-dioxygenase (A), cyclooxygenase-2 (B), inducible nitric oxide synthase (C), transforming growth factor- β (D), hepatocyte growth factor (E), and vascular endothelial growth factor (F) was determined by real-time polymerase chain reaction. Each bar represents the mean \pm SD from four determinations. Abbreviations: Ad-MSC, adipose tissue-derived mesenchymal stem cell; BM-MSC, bone marrow-derived mesenchymal stem cell; LPS, lipopolysaccharide; LSC, limbal epithelial stem cell.

in untreated corneas and in corneas treated with cell-free nanofiber scaffolds. In corneas treated with Ad-MSC-seeded nanofiber scaffolds, the corneal thickness slightly decreased, but it was significantly reduced already on day 5 in corneas treated with nanofiber scaffolds seeded with BM-MSCs or LSCs (Fig. 4). On day 12 after injury, the corneal thickness remained enhanced in untreated injured corneas but was significantly decreased in corneas treated with cell-free or Ad-MSC-seeded nanofiber scaffolds. In corneas treated with nanofiber scaffolds seeded with BM-MSCs or LSCs, the corneal thickness returned to the values observed before injury (Fig. 4).

Expression of VEGF and Neovascularization in Injured and Stem Cell-Treated Corneas

The expression of VEGF was very low in healthy control corneas (Fig. 5A). On day 12 after the injury, the expression of VEGF was high in untreated corneas (Fig. 5B) and was only slightly decreased in corneas treated with cell-free nanofiber scaffolds (Fig. 5C). The treatment of injured corneas with Ad-MSC-seeded nanofiber scaffolds apparently reduced VEGF expression (Fig. 5E), but the greatest reduction in VEGF expression was seen in corneas treated with nanofiber scaffolds seeded with BM-MSCs (Fig. 5D) or LSCs (Fig. 5F). The quantification of corneal neovascularization is summarized in Figure 5H. The number of vessels was high in untreated

injured corneas and was partially reduced in injured corneas treated with cell-free nanofibers. The treatment of injured corneas with nanofiber scaffolds seeded with all three types of stem cells significantly decreased neovascularization. The greatest decrease was found in injured corneas treated with nanofiber scaffolds seeded with BM-MSCs or LSCs.

Corneal Re-epithelialization After Treatment of Injured Eyes With MSCs or LSCs

The extent of corneal re-epithelialization was evaluated on day 12 after alkali injury by examining corneal sections stained with mAb anti-K3/K12. A typical image of a normal healthy cornea is shown in Figure 6A. In contrast, only rare and isolated islands of the epithelium were detected in untreated injured corneas (Fig. 6B). Covering the injured ocular surface with a cell-free nanofiber scaffold improved re-epithelialization and islands with epithelium covered about 20%–40% of the corneal surface (Fig. 6C, 6D). The transfer of stem cell-seeded nanofiber scaffolds onto the damaged ocular surface (Figs. 6E–6G) significantly improved corneal healing, with the best re-epithelialization observed in corneas treated with nanofiber scaffolds seeded with BM-MSCs (Fig. 6E) or LSCs (Fig. 6G). The expression of genes for the cytokeratins K3 and K12 in healthy, injured and treated corneas was

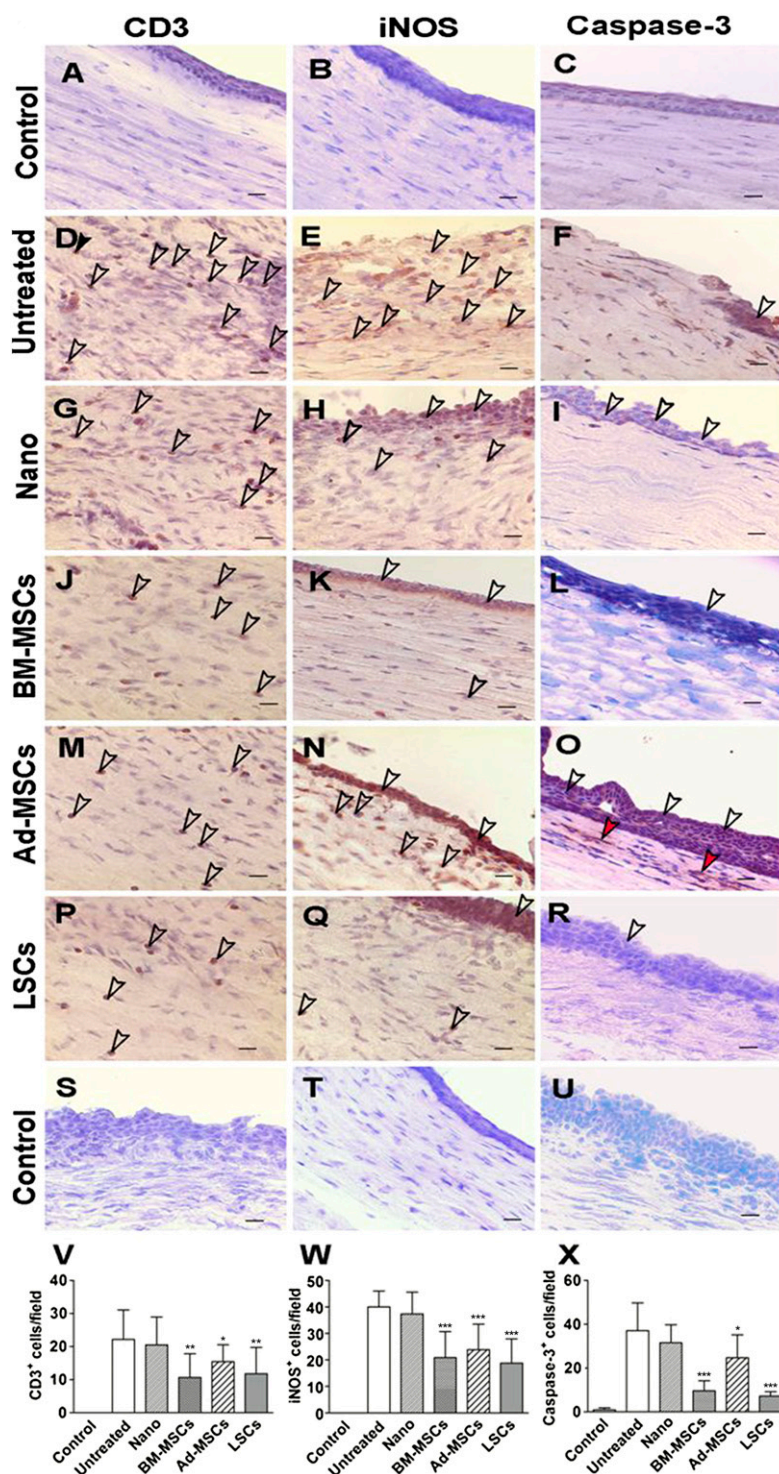


Figure 3. The immunohistochemical detection of CD3⁺, iNOS⁺, and caspase-3⁺ cells in healthy, injured and stem cell-treated corneas. (A–C): Undetectable or very low numbers of CD3⁺ (A), iNOS⁺ (B), or caspase-3⁺ (C) cells were found in healthy corneas. (D–I): On day 12 after alkali injury, the number of CD3⁺ (D), iNOS⁺ (E), and apoptotic caspase-3⁺ (F) cells was significantly increased and remained high in corneas treated with a cell-free nanofiber scaffold (G–I). (J, M, P): The presence of CD3⁺ cells was clearly decreased in corneas treated with nanofiber scaffolds seeded with BM-MSCs (J), Ad-MSCs (M), or LSCs (P). (K, N, Q): Similarly, the number of iNOS⁺ cells was decreased in corneas treated with BM-MSCs (K), Ad-MSCs (N), or LSCs (Q). (L, O, R): The presence of caspase-3⁺ cells, which were numerous in the remaining islands of the corneal epithelium in untreated injured corneas, was decreased in the corneas treated with BM-MSCs (L), Ad-MSCs (O), or LSCs (R). (S–U): Cells expressing CD3 (S), iNOS (T), or caspase-3 (U) were absent in corneal sections stained only with counterstaining, where the primary antibody was omitted from the incubation medium (negative control). Scale bars = 50 μ m. (V–X): The numbers of CD3⁺ (V), iNOS⁺ (W), and caspase-3⁺ (X) cells counted in comparable fields of corneal sections were determined from six corneas in the individual experimental groups. The values with asterisks are significantly different (*, $p < .05$; **, $p < .01$; ***, $p < .001$) from those of untreated injured corneas. Abbreviations: Ad-MSC, adipose tissue-derived mesenchymal stem cell; BM-MSC, bone marrow-derived mesenchymal stem cell; iNOS, inducible nitric oxide synthase; LSC, limbal epithelial stem cell; nano, nanofiber scaffold.

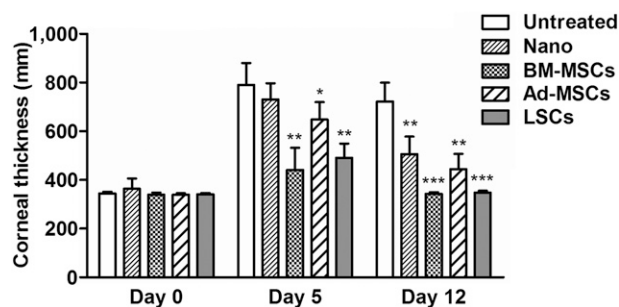


Figure 4. Central corneal thickness of healthy, alkali-injured and stem cell-treated corneas. The corneas were injured with alkali and then left untreated, treated with a nanofiber scaffold alone or treated with nanofiber scaffolds seeded with BM-MSCs, Ad-MSCs, or LSCs. The central corneal thickness was measured in the same rabbit before injury (day 0) and on days 5 and 12 after the injury. Each bar represents the mean \pm SD from six corneas. The values with asterisks for day 5 are significantly different from those of untreated injured corneas on day 5; similarly, the values with asterisks for day 12 are significantly different from those of untreated injured corneas on day 12 (*, $p < .05$; **, $p < .01$; ***, $p < .001$). Abbreviations: Ad-MSC, adipose tissue-derived mesenchymal stem cell; BM-MSC, bone marrow-derived mesenchymal stem cell; LSC, limbal epithelial stem cell; nano, nanofiber scaffold.

quantified by real-time PCR (Fig. 6I, 6J). Cytokeratin gene expression was apparent in healthy corneas but was absent or very low in untreated injured corneas and in corneas treated with cell-free nanofiber scaffolds. In accordance with the immunohistochemical results, the treatment of injured corneas with BM-MSC- or LSC-seeded nanofiber scaffolds significantly enhanced the expression of both cytokeratin genes.

Corneal Opacity of Alkali-Injured and Stem Cell-Treated Eyes

Representative photographs of healthy, injured and treated eyes are shown in Figure 7. In comparison with healthy control eyes (Fig. 7A), the corneas of injured eyes became opalescent shortly after the injury and remained opalescent and highly vascularized on day 12 after injury (Fig. 7C). An eye on day 2 after injury and covered with a nanofiber scaffold is shown in Figure 7B. Only a weak improvement in the appearance of the corneas was observed on day 12 in the eyes treated with cell-free nanofiber scaffolds (Fig. 7D). In the eyes treated with stem cell-seeded nanofibers, corneal opacity was decreased and corneal neovascularization was less apparent (Fig. 7E–7G), with the best therapeutic effects seen with nanofiber scaffolds seeded with BM-MSCs (Fig. 7E) or LSCs (Fig. 7G).

DISCUSSION

Stem cell-based therapy holds great promise for the treatment of severe injuries as well as a number of thus-far incurable diseases. The best source of stem cells for tissue therapy is tissue-specific stem cells, but these cells are often rare in the body, difficult to isolate, and not easily handled in vitro. Therefore, research is focused on the search for alternative cell sources that could effectively replace tissue-specific stem cells.

One possibility has been offered by embryonic stem cells (ESCs), but the use of ESCs is limited by their uncontrolled growth, the risk of teratoma formation, and ethical problems associated with their isolation and use [25, 26]. Induced pluripotent stem cells, which could be used as autologous cells, initially appeared to offer great promise, but

these cells turned out to be immunogenic even in syngeneic hosts [27] and frequently form teratomas after in vivo application [28]. MSCs represent a convenient type of stem cells with a wide spectrum of potential applications. These cells can be obtained in relatively sufficient numbers from an individual patient, can be easily propagated in vitro, and can then be used as autologous cells without requiring immunosuppression after their transplantation.

To treat ocular surface injuries or various types of LSCD, LSCs represent the optimal cell source, and LSC transplantation has resulted in the recovery of vision in blind patients [4, 6, 29]. However, the use of LSCs is limited by the absence of autologous LSCs in the case of bilateral LSCD and by a requirement for strong immunosuppression if allogeneic LSCs are used. To overcome these limitations, attempts have been made to use other cell sources for ocular surface regeneration, and the results of experimental studies using various cell types to treat LSCD have been published [30–32], but the majority of these studies have used MSCs [12, 17–19]. The rationale for the use of MSCs is based on their ability to differentiate into various cell types even apart from the mesodermal lineage from which they originate [7, 9], to produce numerous growth and trophic factors [33], and to inhibit harmful inflammatory reactions [12, 17]. Although an apparent improvement of corneal healing after the application of MSCs has been observed in various models, a direct comparison of the therapeutic effects of MSCs and LSCs has not previously been made.

In this study, we prepared BM-MSCs, Ad-MSCs, and LSCs always from the same rabbit and we compared their growth, differentiation properties, and ability to produce immunoregulatory and growth factors and to support the healing of the damaged ocular surface. All of these cell types have similar fibrocytic morphology and comparable growth characteristics. After cultivation in adipogenic differentiation medium, the highest differentiation potential was observed in BM-MSCs. In accordance with the literature data [33–35], all three types of stem cells spontaneously, or after stimulation with LPS, expressed genes for a number of immunoregulatory and growth factors, but the secretion profiles were different among the individual cell types. Though we were not able to characterize the stem cell populations phenotypically because of the lack of species-specific antibodies for the rabbit model, our MSCs fulfilled other criteria for MSCs: their morphology, adherence to plastic, differentiation, and factor production [36]. Similarly, the population of LSCs was prepared by a standard method described for the preparation of mouse [20], rat [9], rabbit [37, 38], or human [5, 6] LSCs. We are aware that the LSC population contains a significant proportion of descendants of LSCs, such as transient corneal epithelial cells and corneal epithelial cells, in addition to LSCs. Indeed, we observed a gradual increase in CK3/CK12 expression during culture of rabbit LSCs (unpublished observation). Some reports suggest that MSCs can be expanded from the limbal tissue in vitro rather than corneal epithelial cells [39, 40]. For example, Basu et al. [40] described the expansion of mesenchymal stromal cells derived from human limbal biopsies and their use for the treatment of mouse corneal wounds. These authors also showed that the type of enzymatic digestion influences the preferential growth of cells with epithelial or mesenchymal morphologies. Thus, there may be species-specific and cell culture-dependent differences that support preferential growth of limbal MSCs or corneal epithelial cells.

We have shown previously in the mouse model that MSCs transferred onto the damaged ocular surface, using a nanofiber scaffold, migrate from the scaffold onto the ocular surface and inhibit the local inflammatory reaction [21]. In the present study, we used a model

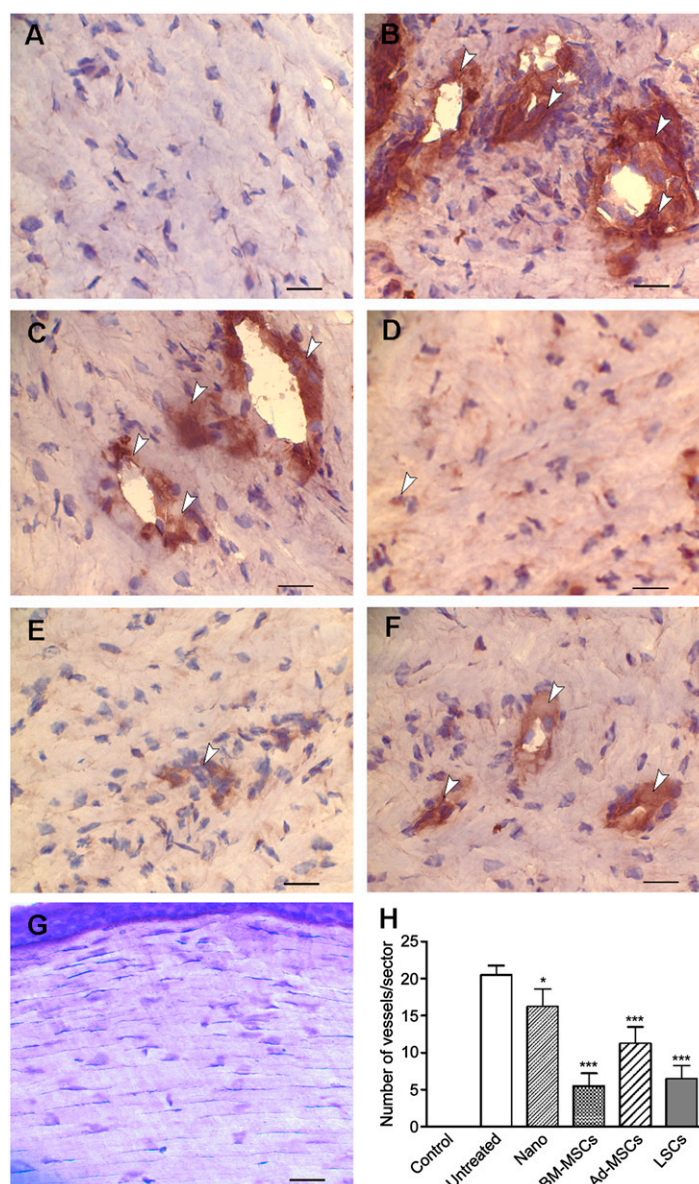


Figure 5. The expression of vascular endothelial growth factor (VEGF) and corneal neovascularization after alkali injury and treatment with stem cell-seeded nanofiber scaffolds. **(A–F):** The expression of VEGF was determined by immunohistochemistry in healthy corneas **(A)** and in alkali-injured corneas on day 12 that were untreated **(B)**, treated with cell-free nanofibers **(C)**; or treated with nanofiber scaffolds seeded with BM-MSCs **(D)**, Ad-MSCs **(E)**, or LSCs **(F)**. **(G):** In the negative control, the sections were stained only with counterstaining (hematoxylin). Scale bars = 10 μ m. **(H):** The quantification of corneal neovascularization was performed by counting the number of vessels in defined corneal sectors. Each bar represents the mean \pm SD from six corneas. The values with asterisks are significantly different (*, $p < .05$; ***, $p < .001$) from those determined in untreated injured corneas. Abbreviations: Ad-MSC, adipose tissue-derived mesenchymal stem cell; BM-MSC, bone marrow-derived mesenchymal stem cell; LSC, limbal epithelial stem cell; nano, nanofiber scaffold.

of the alkali-injured ocular surface in rabbits and compared the therapeutic potential of two types of MSCs and tissue-specific LSCs. The injury of the cornea with 0.25N NaOH induced damage of the corneal epithelium, an increase in corneal thickness, a strong infiltration with cells of adaptive (T lymphocytes) and innate (iNOS-expressing cells) immunity, an increase in the presence of apoptotic cells (caspase-3⁺ cells), neovascularization, and corneal opacity associated with decreased corneal transparency. All these parameters characterizing the ocular injury were decreased in the treated eyes. The nanofiber scaffold itself

slightly supported healing and decreased the harmful impacts of injury, similarly to what has been described after the treatment of injured eyes with a nanofiber scaffold seeded with stem cells significantly decreased all of the harmful manifestations of the injury. The alkali injury strongly damaged the corneal epithelium (as demonstrated by immunohistochemistry and real-time PCR for K3 and K12), and treatment with a stem cell-seeded nanofiber scaffold improved re-epithelialization. The less-pronounced therapeutic effects of Ad-MSCs in comparison with

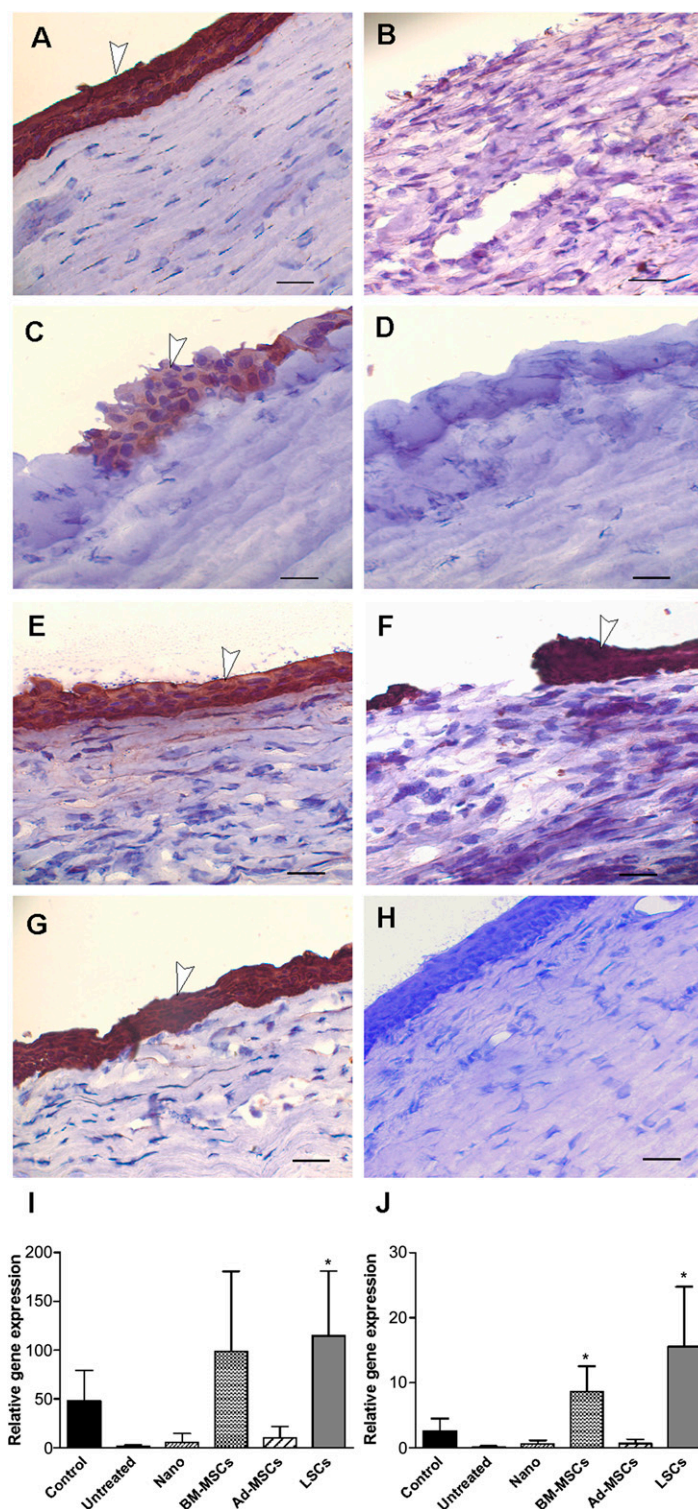


Figure 6. Corneal re-epithelialization in alkali-injured and stem cell-treated corneas. **(A–G):** The individual photographs show representative images of an anti-K3/12 stained healthy cornea **(A)**, an untreated injured cornea **(B)**, or injured corneas treated with cell-free nanofibers **(C, D)**, nanofibers seeded with BM-MSCs **(E)**, Ad-MSCs **(F)**, or LSCs **(G)**. All injured corneas are shown on day 12 after injury. **(H):** The staining for the cytokeratins K3/12 was negative in corneal sections stained only with counterstaining, where the primary antibody was omitted from the incubation medium. Scale bars = 50 μm . **(I, J):** The expression of genes for K3 **(I)** and K12 **(J)** in individual experimental groups on day 12 after injury was determined by real-time polymerase chain reaction. Each bar represents the mean \pm SD from six individual corneas. The values with an asterisk represent a statistically significant ($p < .05$) difference from the values determined in untreated injured corneas. Abbreviations: Ad-MSC, adipose tissue-derived mesenchymal stem cell; BM-MSC, bone marrow-derived mesenchymal stem cell; LSC, limbal epithelial stem cell; nano, nanofiber scaffold.

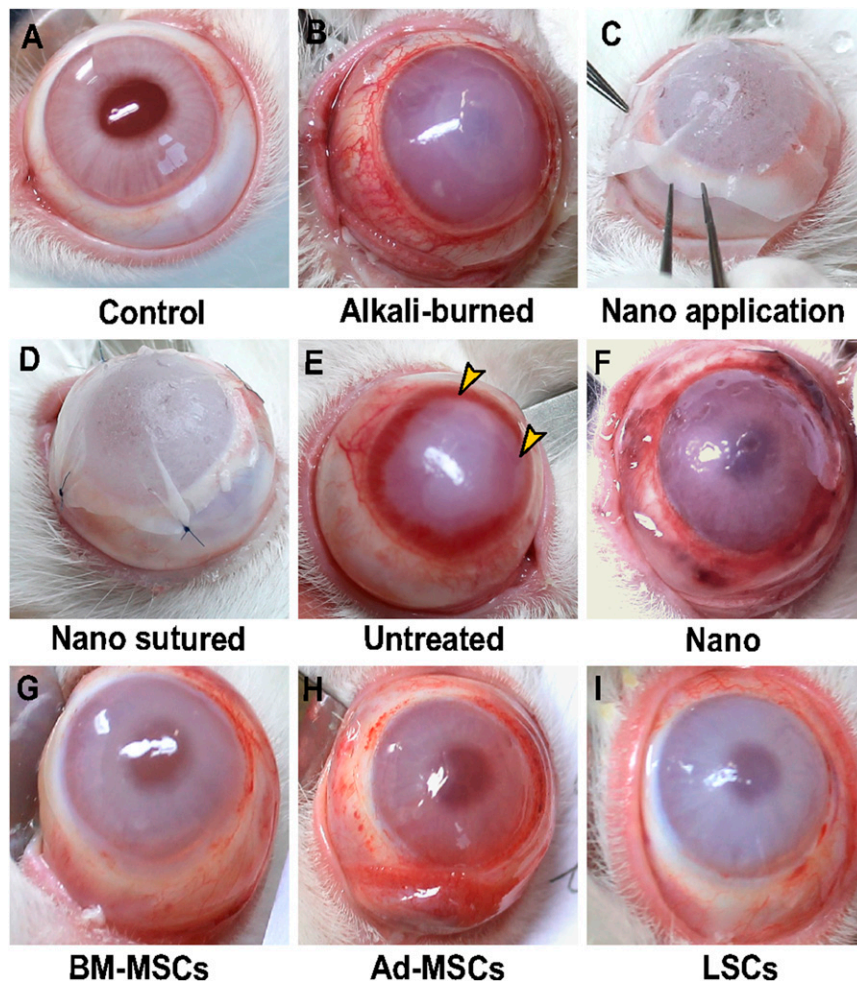


Figure 7. Corneal opacity of alkali-injured and stem cell-treated eyes. Representative photographs show a healthy control eye (A), an alkali-injured eye (immediately after the injury) (B), an injured eye with nanofiber application (C), and a sutured nanofiber scaffold (immediately after the injury) (D); and injured eyes on day 12 that were either untreated (E), treated with a cell-free nanofiber scaffold (F), or treated with nanofiber scaffolds seeded with BM-MSCs (G), Ad-MSCs (H), or LSCs (I). (E, G, I): Corneal neovascularization was clearly visible expressed in untreated injured corneas (E, arrows) and strongly suppressed in corneas treated with nanofiber scaffolds seeded with BM-MSCs (G) or LSCs (I). Abbreviations: Ad-MSC, adipose tissue-derived mesenchymal stem cell; BM-MSC, bone marrow-derived mesenchymal stem cell; LSC, limbal epithelial stem cell; nano, nanofiber scaffold.

BM-MSCs or LSCs could be due to the lower differentiation potential of Ad-MSCs and to the different spectrum of growth and immunoregulatory factors produced by these cells.

CONCLUSION

Taken together, our results show that BM-MSCs have comparable therapeutic effects to those of tissue-specific LSCs on the healing of corneal injury. Even though there are data on the direct differentiation of MSCs into corneal epithelial cells [8, 18], this transdifferentiation is probably not the main mechanism of the healing effect of MSCs [42]. We suggest that a more important role is represented by the production of numerous trophic and growth factors that can support the growth of residual corneal epithelial cells and LSCs [33–35], and by the ability of MSCs to suppress the local inflammatory reaction that could impede the healing process [12, 43]. All of these properties make BM-MSCs a promising candidate cell population for improving ocular surface healing in situations when autologous LSCs are difficult to obtain or are absent.

ACKNOWLEDGMENTS

This work was supported by Grant 14-12580S from the Grant Agency of the Czech Republic, Grant NT/14102 from the Grant Agency of the Ministry of Health of the Czech Republic, Grants 889113 and 80815 from the Grant Agency of the Charles University, and Projects Biocev CZ.1.05/1.1.00/02.0109, NPU1: LO1309, UNCE 204013, and SVV 260206.

AUTHOR CONTRIBUTIONS

V.H.: conception and design, financial support, manuscript writing; P.T., E.J., B.H., and M.C.: collection and/or assembly of data; C.C. and A.Z.: collection of data, data analysis and interpretation; J.C.: conception and design, collection and/or assembly of data, manuscript writing.

DISCLOSURE OF POTENTIAL CONFLICTS OF INTEREST

The authors indicated no potential conflicts of interest.

REFERENCES

- 1 Tan DT, Ficker LA, Buckley RJ. Limbal transplantation. *Ophthalmology* 1996;103:29–36.
- 2 Dua HS, Azuara-Blanco A. Allo-limbal transplantation in patients with limbal stem cell deficiency. *Br J Ophthalmol* 1999;83:414–419.
- 3 Cauchi PA, Ang GS, Azuara-Blanco A et al. A systematic literature review of surgical interventions for limbal stem cell deficiency in humans. *Am J Ophthalmol* 2008;146:251–259.
- 4 Rama P, Matuska S, Paganoni G et al. Limbal stem-cell therapy and long-term corneal regeneration. *N Engl J Med* 2010;363:147–155.
- 5 Marchini G, Pedrotti E, Pedrotti M et al. Long-term effectiveness of autologous cultured limbal stem cell grafts in patients with limbal stem cell deficiency due to chemical burns. *Clin Experiment Ophthalmol* 2012;40:255–267.
- 6 Basu S, Ali H, Sangwan VS. Clinical outcomes of repeat autologous cultivated limbal epithelial transplantation for ocular surface burns. *Am J Ophthalmol* 2012;153:643–650, 650.e1–650.e2.
- 7 Pittenger MF, Mackay AM, Beck SC et al. Multilineage potential of adult human mesenchymal stem cells. *Science* 1999;284:143–147.
- 8 Gu S, Xing C, Han J et al. Differentiation of rabbit bone marrow mesenchymal stem cells into corneal epithelial cells in vivo and ex vivo. *Mol Vis* 2009;15:99–107.
- 9 Jiang TS, Cai L, Ji WY et al. Reconstruction of the corneal epithelium with induced marrow mesenchymal stem cells in rats. *Mol Vis* 2010;16:1304–1316.
- 10 Reinshagen H, Auw-Haedrich C, Sorg RV et al. Corneal surface reconstruction using adult mesenchymal stem cells in experimental limbal stem cell deficiency in rabbits. *Acta Ophthalmol* 2011;89:741–748.
- 11 Holan V, Javorkova E. Mesenchymal stem cells, nanofiber scaffolds and ocular surface reconstruction. *Stem Cell Rev* 2013;9:609–619.
- 12 Cejkova J, Trosan P, Cejka C et al. Suppression of alkali-induced oxidative injury in the cornea by mesenchymal stem cells growing on nanofiber scaffolds and transferred onto the damaged corneal surface. *Exp Eye Res* 2013;116:312–323.
- 13 Holan V, Pokorna K, Prochazkova J et al. Immunoregulatory properties of mouse limbal stem cells. *J Immunol* 2010;184:2124–2129.
- 14 Di Trapani M, Bassi G, Ricciardi M et al. Comparative study of immune regulatory properties of stem cells derived from different tissues. *Stem Cells Dev* 2013;22:2990–3002.
- 15 Strioga M, Viswanathan S, Darinskas A et al. Same or not the same? Comparison of adipose tissue-derived versus bone marrow-derived mesenchymal stem and stromal cells. *Stem Cells Dev* 2012;21:2724–2752.
- 16 Jin HJ, Bae YK, Kim M et al. Comparative analysis of human mesenchymal stem cells from bone marrow, adipose tissue, and umbilical cord blood as sources of cell therapy. *Int J Mol Sci* 2013;14:17986–18001.
- 17 Oh JY, Kim MK, Shin MS et al. The anti-inflammatory and anti-angiogenic role of mesenchymal stem cells in corneal wound healing following chemical injury. *STEM CELLS* 2008;26:1047–1055.
- 18 Ma Y, Xu Y, Xiao Z et al. Reconstruction of chemically burned rat corneal surface by bone marrow-derived human mesenchymal stem cells. *STEM CELLS* 2006;24:315–321.
- 19 Yao L, LiZR, Su WR et al. Role of mesenchymal stem cells on cornea wound healing induced by acute alkali burn. *PLoS One* 2012;7:e30842.
- 20 Krulova M, Pokorna K, Lencova A et al. A rapid separation of two distinct populations of mouse corneal epithelial cells with limbal stem cell characteristics by centrifugation on percoll gradient. *Invest Ophthalmol Vis Sci* 2008;49:3903–3908.
- 21 Zajicova A, Pokorna K, Lencova A et al. Treatment of ocular surface injuries by limbal and mesenchymal stem cells growing on nanofiber scaffolds. *Cell Transplant* 2010;19:1281–1290.
- 22 Svobodova E, Krulova M, Zajicova A et al. The role of mouse mesenchymal stem cells in differentiation of naive T-cells into anti-inflammatory regulatory T-cell or proinflammatory helper T-cell 17 population. *Stem Cells Dev* 2012;21:901–910.
- 23 Holan V, Chudickova M, Trosan P et al. Cyclosporine A-loaded and stem cell-seeded electrospun nanofibers for cell-based therapy and local immunosuppression. *J Control Release* 2011;156:406–412.
- 24 Trosan P, Svobodova E, Chudickova M et al. The key role of insulin-like growth factor I in limbal stem cell differentiation and the corneal wound-healing process. *Stem Cells Dev* 2012;21:3341–3350.
- 25 Gong SP, Kim B, Kwon HS et al. The coinjection of somatic cells with embryonic stem cells affects teratoma formation and the properties of teratoma-derived stem cell-like cells. *PLoS One* 2014;9:e105975.
- 26 Bobbert M. Ethical questions concerning research on human embryos, embryonic stem cells and chimeras. *Biotechnol J* 2006;1:1352–1369.
- 27 Zhao T, Zhang ZN, Rong Z et al. Immunogenicity of induced pluripotent stem cells. *Nature* 2011;474:212–215.
- 28 Nishimori M, Yakushiji H, Mori M et al. Tumorigenesis in cells derived from induced pluripotent stem cells. *Hum Cell* 2014;27:29–35.
- 29 Pellegrini G, Rama P, Di Rocco A et al. Concise review: hurdles in a successful example of limbal stem cell-based regenerative medicine. *STEM CELLS* 2014;32:26–34.
- 30 Inatomi T, Nakamura T, Kojyo M et al. Ocular surface reconstruction with combination of cultivated autologous oral mucosal epithelial transplantation and penetrating keratoplasty. *Am J Ophthalmol* 2006;142:757–764.
- 31 Gomes JA, Gerales Monteiro B, Melo GB et al. Corneal reconstruction with tissue-engineered cell sheets composed of human immature dental pulp stem cells. *Invest Ophthalmol Vis Sci* 2010;51:1408–1414.
- 32 Liu H, Zhang J, Liu CY et al. Cell therapy of congenital corneal diseases with umbilical mesenchymal stem cells: lumican null mice. *PLoS One* 2010;5:e10707.
- 33 Oh JY, Kim MK, Shin MS et al. Cytokine secretion by human mesenchymal stem cells cocultured with damaged corneal epithelial cells. *Cytokine* 2009;46:100–103.
- 34 Di Nicola M, Carlo-Stella C, Magni M et al. Human bone marrow stromal cells suppress T-lymphocyte proliferation induced by cellular or nonspecific mitogenic stimuli. *Blood* 2002;99:3838–3843.
- 35 Najar M, Raicevic G, Fayyad-Kazan H et al. Immune-related antigens, surface molecules and regulatory factors in human-derived mesenchymal stromal cells: the expression and impact of inflammatory priming. *Stem Cell Rev* 2012;8:1188–1198.
- 36 Dominici M, Le Blanc K, Mueller I et al. Minimal criteria for defining multipotent mesenchymal stromal cells. The International Society for Cellular Therapy position statement. *Cytotherapy* 2006;8:315–317.
- 37 Wan P, Wang X, Ma P et al. Cell delivery with fixed amniotic membrane reconstructs corneal epithelium in rabbits with limbal stem cell deficiency. *Invest Ophthalmol Vis Sci* 2011;52:724–730.
- 38 Samoilă O, Soroiță O, Totu L et al. Cultivation and characterization of limbal epithelial stem cells in rabbits. *Rom J Morphol Embryol* 2014;55:63–69.
- 39 Polisetty N, Fatima A, Madhira SL et al. Mesenchymal cells from limbal stroma of human eye. *Mol Vis* 2008;14:431–442.
- 40 Basu S, Hertszenberg AJ, Funderburgh ML et al. Human limbal biopsy-derived stromal stem cells prevent corneal scarring. *Sci Transl Med* 2014;6:266ra172.
- 41 Dubský M, Kubínová S, Sirc J et al. Nanofibers prepared by needleless electrospinning technology as scaffolds for wound healing. *J Mater Sci Mater Med* 2012;23:931–941.
- 42 Harkin DG, Foyn L, Bray LJ et al. Concise reviews: Can mesenchymal stromal cells differentiate into corneal cells? A systematic review of published data. *STEM CELLS* 2015;33:785–791.
- 43 Abumaree M, Al Jumah M, Pace RA et al. Immunosuppressive properties of mesenchymal stem cells. *Stem Cell Rev* 2012;8:375–392.